

Ivar Østby · Ragnar Winther

Stability of a model of human granulopoiesis using continuous maturation

Received: 24 June 2003 / Revised version: 11 December 2003 /

Published online: 5 July 2004 – © Springer-Verlag 2004

Abstract. A class of mathematical models involving a convection-reaction partial differential equation (PDE) is introduced with reference to recovering human granulopoiesis after high dose chemotherapy with stem cell support. The stability properties of the model are addressed by means of numerical investigations and analysis. A simplified model with proliferation rate and mobilization rate independent of maturity shows that the model is stable as the maturation rate grows without bounds, but may go through stable and non-stable regimens as the maturation rate varies. It is also shown that the system is stable when parameters are chosen to approximate a real physiological situation.

System characteristics do not change profoundly by introduction of a maturity-dependent proliferation and mobilization rate, as is necessary to make the model operate more in accordance with hematological observations. However, by changing the system mitotic responsiveness with respect to changes in cytokine level, the system is still stable but may show persistent oscillations much resembling clinical observations of cyclic neutropenia. Furthermore, in these cases, changes in the model feedback signal caused by, for instance, an impaired effective cytokine elimination by cell receptors may enforce these oscillations markedly.

1. Introduction

Convection-reaction PDE models, commonly used to describe propagation of waves in a medium, may also be used as models of cell proliferation and maturation. In the last case, wave propagation along a physical axis has to be replaced by cell development on a maturation scale with maturation rate taking the place of the analogous wave velocity.

The class of convection-reaction PDE models used in the present work originated as an example of a continuous mathematical model for the development of neutrophilic granulocytes, i.e. an important kind of white blood cells being produced in the vertebrate bone marrow. The model was used to solve a modeling problem concerning high-dose chemotherapy with stem cell support [41]. The model describes the evolution of cell density as a function of maturity, and was chosen as a simple way of describing a possible relation between the number of

I. Østby: Department of Informatics, University of Oslo, Box 1080, Blindern, 0316 Oslo, Norway. e-mail: ivaro@ifi.uio.no

R. Winther: Centre of Mathematics for Applications (CMA) and Department of Informatics, Box 1080, Blindern, 0316 Oslo, Norway. e-mail: rwinther@ifi.uio.no

Key words or phrases: Stability – Granulopoiesis – Mathematical model

certain immature progenitor cells given as autotransplant to the patient and the time needed for reconstitution of the granulopoietic system. In contrast to compartment models also used to describe the evolution of granulocytes [30],[31],[32],[33],[34], the basis for the present model is the concept of continuous maturing, i.e. maturing of neutrophil pre-stages (progenitors and precursors) takes place on a continuous scale. The appearance of a PDE model is a consequence of the introduction of this concept.

The present work focuses on the stability properties of such a model. Furthermore, certain conditions for the existence of cyclic solutions of the model are shown and discussed.

Continuous mathematical models of cell proliferation and maturation have been used to gain insight into numerical evaluation of various cell lineages [38], cell regeneration after neutropenia [27], and the regulation of cell production in a specific cell lineage [14], [15], [18], [20], [23], [24], [25], [30], [31], [32], [33], [34], [35], [36], [39].

Common to such models is a feedback mechanism linking the level of endogenous cytokines (signal-transmitting substances) to the cell proliferation. Cytokines (like, for instance, granulocyte colony stimulating factor (G-CSF) or granulocyte-macrophage colony stimulating factor (GM-CSF) for the granulocytes) are produced by certain cells in the body (monocytes, macrophages) and will act as signal mediators designed to speed up cell production if the cell supply in the bone marrow and blood is scarce. As a substantial number of cells is being produced, cytokines are eliminated by cell receptors, thereby diminishing the overall cytokine level available and resulting in a slower production. In this way, the cytokine pathway constitutes a negative feedback loop for cell production.

Due to this feedback effect, the question of stability conditions for the actual mathematical model turns up. Considerable effort has been laid down in order to analyze the origins of instability and find sharp criteria for stability of the models in question. The present work focuses on conditions for stability in the sense that perturbations from the steady state tend to zero as time increases. The conditions for stability were assessed following general principles outlined in the work by MacDonald [21]. In many other texts, the concept of stability is linked to non-cyclic solutions of the equations in question. The pathological condition named cyclical neutropenia is a well-known case where the output cellularity enters a state of periodic fluctuations [4], [10], [16], [40]. In the past, this condition has been analyzed with reference to various mathematical models [6], [12], [13], [14], [15], [18], [22], [23], [24], [25], [26], [27], [28], [30], [31], [32], [35]. The present results concerning cyclic states of the system confirm some of the results of earlier investigators. In particular, the importance of the mitotic responsiveness of the system relative to changes in cytokine concentration was stated by Schmitz et al [30], [31], [32] and Mackey et al [22], [23], [24]. However, the present work shows that the mitotic responsiveness is important not only for the existence of cyclic output solutions, but also for the stability in the sense mentioned above. Furthermore, we point out that a second potential reason for cyclic solutions may be an altered maturity distribution of cells participating in G-CSF elimination or an extensive cell death.

Recent modeling by Haurie et al [12], [13], [14], [15] indicates that a probable explanation of cyclic blood neutrophil counts may be found in cyclic variations at a stem cell level due to a defective autoregulation at this level. As a consequence of the present results, it may be argued that a defective G-CSF feedback loop from later maturity stages back to progenitor levels leads to a similar effect.

The aims of the present investigation are as follows:

- 1) To give reasons for system stability under ordinary conditions,
- 2) To give conditions for transitions from stable to unstable states,
- 3) To give conditions for transitions to stable cyclic states,
- 4) To give physiological interpretations of the conditions found.

2. Model of recovering granulopoiesis after high dose chemotherapy with stem cell support

2.1. Biological system

The neutrophilic granulocytes, a special kind of white blood cells constituting the first line of defence against intruding microbes, belong to the group of myeloid blood cells. Figure 1 shows a schematic representation of the development of the myeloid blood cells. HSC symbolizes the hematopoietic stem cells, differentiating into lymphoid and myeloid progenitor cells. Myeloid progenitor cells include the LTC-IC (long-term culture initiating cells) and the CFU-GM (colony forming unit granulocyte macrophage) cells. The latter ones initiate the granulocyte and macrophage cell lineages. The maturing time from the LTC-IC to the CFU-GM stage is of the order of 5–8 weeks. Specific progenitor cells may be recognized or separated by using monoclonal antibodies fitting with specific antigens on the cell surface. The antibody CD34 reacts with the hematopoietic progenitor cells and is used as a marker. Accordingly, these progenitor cells are named CD34+ cells. CD34+ cells constitute about 0.5 to 5 % of normal bone marrow and less than 1 % of peripheral blood nucleated cells. The neutrophilic granulocytes constitute the major part

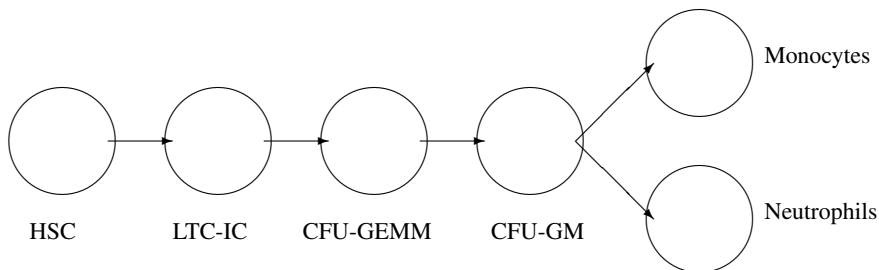


Fig. 1. Development of the myeloid blood cells.

HSC = Hematopoietic stem cell, LTC-IC = Long-term culture initiating cells, CFU-GEMM = Colony forming unit granulocyte erythroid macrophage megakaryocyte, CFU-GM = Colony forming unit granulocyte macrophage.

(about 70 %) of the white blood cells (leukocytes). When leaving the bone marrow, mature neutrophils are mobilized to the circulating blood or to the margined pool. Margined neutrophils are thought to reside in the lung capillaries, the walls of venules, in the liver, and the spleen. Every day, the bone marrow produces some $7 \cdot 10^{11}$ granulocytes. In the circulating blood, their half-life is about 7 hours.

2.2. *Clinical problem*

Cancer patients exposed to high dose chemotherapy will experience a period of many days where the number of living blood cells is reduced to a minimum. Since this applies also to white blood cells, constituting the first line of defence against intruding microbes, the patients run the risk of getting fatal infections. The patients in question are given stem cell support, i.e., they are transplanted with a concentrated blood product containing some of their own stem and progenitor cells which were extracted from the blood prior to chemotherapy. The transplanted cell graft, enriched in CD34+ cells [19], will proliferate and eventually repopulate the bone marrow and reconstitute a normal content of blood cells. These include the neutrophilic granulocytes which constitute about 70 % of all white blood cells. The object of a former work [41] was to use a mathematical model to investigate a possible correlation between the number of CFU-GM cells reinfused and the length of the period with practically no living granulocytes in the blood (the neutropenic period, often measured by means of the engraftment time, i.e. the time for the level of blood granulocytes to reach a concentration of $0.5 \cdot 10^9$ cells/liter blood). The model uses a convection-reaction partial differential equation with feedback from a secondary compartment modeling the endogenous level of the cytokine G-CSF. Normally, G-CSF is produced by monocytes and macrophages and is eliminated by means of receptors on the cell surface of neutrophilic granulocytes. Potentially, G-CSF has the ability to speed up neutrophil proliferation, reduce the risk of cell death, and increase mobilization from the bone marrow to the blood.

The clinical problem so described offers an opportunity to study the granulopoietic system as it starts up from a state of practically zero level of granulocytes. This means that the model must include an initial condition given as the cell density as a function of maturity. This initial condition was constructed according to an assumption of how the proliferation rate of the reinfused CD34+ cells may be distributed over a maturity scale (Figure 4A, explained below).

2.3. *Model results*

The model gave good estimates of how the concentration of granulocytes in the blood will develop as a function of time after reinfusion of the CD34+ cell product. Figure 2 (A, left-hand figure) shows an example of blood granulocyte concentration data as recorded in a patient (stars) as compared to engraftment data predicted by the model (solid line). Figure 2B (right-hand figure) shows the corresponding model predicted levels of serum G-CSF in the body versus time, indicating a substantial descent in G-CSF levels as increasing numbers of neutrophils contribute to G-CSF

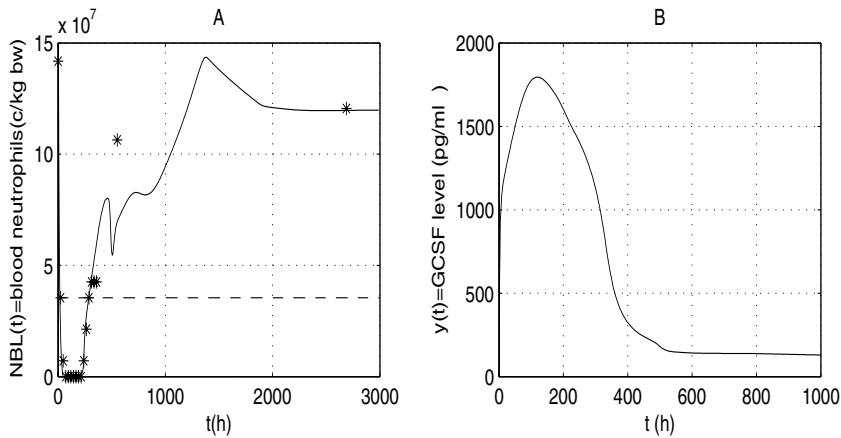


Fig. 2. A): Engraftment data: Neutrophil concentration in the circulating blood vs. time after reinfusion of the concentrated CD34+ blood product. Stars: Patient data observed in one selected patient. Solid line: Model predictions. B): Endogenous serum G-CSF concentration corresponding to engraftment shown in A), calculated by the model.

elimination. For a discussion of the link between model parameters and clinical data, we refer to [41].

The model suggested a firm correspondence between the number of CFU-GM progenitor cells in the reinfused CD34+ cell product and the length of the neutrophenic period. As the reinfused CFU-GM content increased, the model showed that engraftment time may approach an asymptotic value of about 9-10 days which seems to be a theoretical minimum value as long as no additional treatment is given. The long-term level of blood granulocytes, on the other hand, seemed to be correlated with the cell density of early progenitors in the reinfused blood product (prior to the CFU-GM cell stage).

Figure 3 shows model predictions of engraftment time (circles) vs. the CFU-GM content of the reinfused blood graft, together with the observed patient data (stars). The predictions were recorded with parameters fixed at median values after optimal model fittings to five selected patient data sets. The model can be said to catch a main trend in the data: Large engraftment times tend to correspond to low CFU-GM counts. Further data are necessary to better evaluate the model.

In all the cases investigated with the model so far, the modeled engraftment curves as depicted in Figure 2A suggested an apparent system stability as judged by the fact that the curves eventually approach a constant level as time increases. To decide if this always is the case, we may pose the following questions:

- 1) In a situation where the model predicts a clinical outcome as described by the observed engraftment curves, will the model always yield an asymptotically stable output?
- 2) Is it possible for this model to yield cyclic solutions?

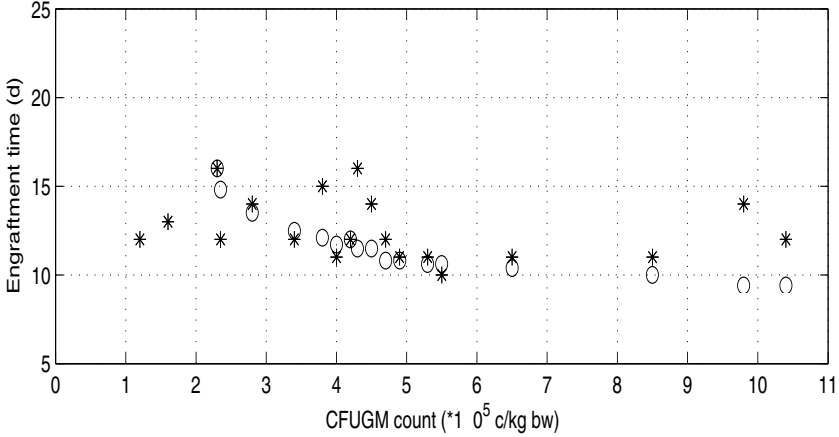


Fig. 3. Engraftment time (time from reinfusion to $0.5 \cdot 10^9$ blood neutrophils/l) vs. CFU-GM content (c/kg bw) in the reinfused blood product. Stars: Observed patient data. Circles: Model predictions.

In the following, it will be shown that a simplified version of the model is stable for physiologically correct values of the parameters, especially a correct value for the maturation rate of neutrophil progenitors and precursors. In this context, by stability is meant that the mean value of the square of a perturbation relative to a steady state solution of the model equations approaches zero with increasing time. As the main simplification, the proliferation rate as well as the mobilization rate from bone marrow to blood were taken to be constants in maturity, i.e. they do not change their values with increasing cell maturity. Also, it will be shown numerically that the original model (with proliferation and mobilization rate taken as proper functions of maturity) may show bifurcations to stable limit cycles by certain choices of parameters, especially parameters deciding the mitotic responsiveness.

2.4. Model details

The original model of recovering granulopoiesis after high dose chemotherapy with stem cell support includes the following generalized equations and conditions:

A convection-reaction PDE for the cell density $u = u(x, t)$ (where x = cell maturity on a scale from 0 to 1, t = time since reinfusion of the CD34+ blood graft):

$$u_t + (\beta u)_x = \alpha u, \quad (1)$$

Here, $u(x, t)$ = cell density, defined by

$$u(x, t) = \frac{\partial N(x, t)}{\partial x},$$

where $N(x, t)$ is the total number of cells in the bone marrow at maturity $\leq x$ and at time t ,

Rates α (proliferation rate), β (maturation rate) are generally functions of maturity x and serum G-CSF concentration $y(t)$:

$$\alpha = \alpha(x, y) \quad \beta = \beta(x, y). \quad (2)$$

Here, the G-CSF level y is a function of t and its evolution is governed by an ordinary differential equation (ODE):

$$y_t = P(y, z) = y_{PROD} - f(y, z) \quad (3)$$

The term y_{PROD} describes the production rate of G-CSF (produced amount of G-CSF per unit time). As a first approximation, the production rate may be assumed constant during the time considered. The function $f(y, z)$ describes the elimination rate of G-CSF by neutrophils and neutrophil progenitors/precursors.

$z = z(t)$ is the effective number of neutrophils participating in the elimination of G-CSF, generally given by a weighted integral of u with respect to x :

$$z(t) = \int_0^1 w(x)u(x, t)dx, \quad (4)$$

Here, $w(x)$ is a general weighting function designed to include the possibility that cells of different maturity contribute differently to the elimination of G-CSF. With $w(x)$ constant equal to 1, $z(t)$ is just the total granulocyte count in the bone marrow.

The function $f(y, z)$ in (3) describing G-CSF elimination was estimated in a former work [41] as:

$$f(y, z) = k_1 y + k_2 z [1 - e^{-\frac{k_3 y}{z+p}}], \quad (5)$$

where k_1, k_2, k_3, p are constant parameters.

Initial and boundary conditions are given by:

$$y(0) = y_0, \quad (6)$$

and for the variable u ,

$$u(x, 0) = u_0(x), \quad (7)$$

$$\beta[0, y(t)]u(0, t) = Q(t), \quad (8)$$

where $Q(t)$ is the input flux to the system due to some earlier stem cell stage not considered in the present model, normally assumed to have a constant value. With all other parameters fixed, its value may be adjusted so as to make the model produce output values of cellularity in accordance with observations.

$u_0(x)$ is the distribution of granulocyte progenitors and precursors in the CD34+ blood cell product transplanted into the patient after the termination of chemotherapy.

A realistic model must include a dependence of maturity x in the expression for α at constant y given in (2), due to the fact that the proliferation rate varies considerably as progenitor cells develop into the more mature stages and proliferation eventually stops at the metamyelocyte stage [1],[5]. Furthermore, the mobilization

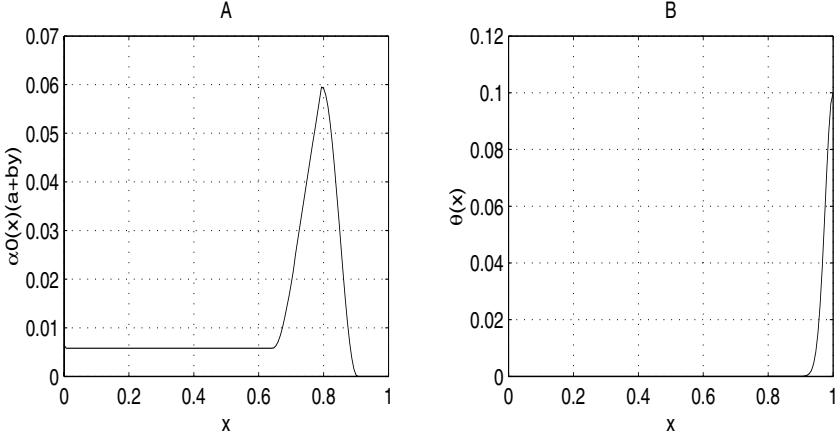


Fig. 4. A): Proliferation rate α_0 vs. maturity x of the reinfused blood graft (9). B): Mobilization rate θ from bone marrow to blood (10) vs. maturity x . Maturity x extends from the LTC-IC progenitor to the mature neutrophil (PMN) stage.

rate θ must vary with maturity since only mature cells are mobilized to blood under ordinary conditions. In the model as described in [41], the net proliferation rate α was made a function of both x (maturity) and y (cytokine (G-CSF) level) by letting

$$\alpha(x, y) = \alpha_0(x)\phi(y) - \theta(x) \quad (9)$$

Here, $\alpha_0(x)$ is a proliferation rate function of x obtained as a piecewise linear function given by considerations of cycle times at progenitor and precursor cell stages. $\phi(y)$ is a saturable, Michaelis-Menten function of the cytokine level y which may be approximated by the linear function $a + by$ for intermediate y levels.

The mobilization rate θ may be modeled by a strictly increasing, polynomial function of x with values close to zero for cell stages prior to the end stages BN and PMN, or, as a simpler approximation, as the sine function

$$\theta(x) = \theta_{max} \sin^n\left(\frac{\pi x}{2}\right). \quad (10)$$

The exponent n decides the maturity distribution of the cells being released from the bone marrow into the blood. A dependence of y giving a left shift of the maturity distribution of blood granulocytes at high y levels [7] may be included also for the θ function, but is omitted here since this only gives effects of small order. Examples of functions $\alpha_0(x)$ and $\theta(x)$ are given in Figure 4 A,B, respectively.

The maturation rate β may also be subject to cytokine control [3]. As shown in [41], a diminished β during the mitotic progenitor and precursor stages will effectively augment net cell proliferation. To simplify the present discussion, this effect has not been included here but may potentially affect system stability.

To obtain an extended system describing the maturation of granulocyte progenitors and precursors, and eventually the mobilization of mature granulocytes from the bone marrow and their appearance in the blood, the system must be completed

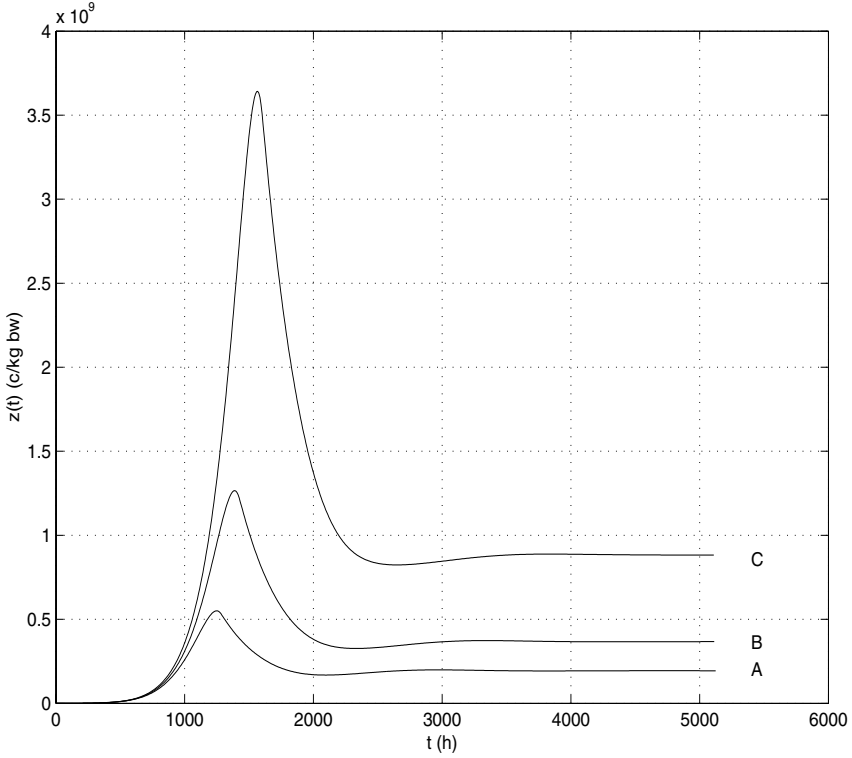


Fig. 5. Output values of $z(t)$ from the simplified main model (16)-(20) for three values of β : A) $\beta = \frac{1}{1281}h^{-1}$ (lower curve), B) $\beta = \frac{1}{1423}h^{-1}$ (middle curve), C) $\beta = \frac{1}{1601}h^{-1}$ (upper curve), suggesting an exponential increase at times $t < \frac{1}{\beta}$ while the system approaches stability when $t > \frac{1}{\beta}$.

with a blood compartment. The content of granulocytes in the blood, NBL , may be calculated from the ordinary differential equation

$$NBL_t = \int_0^1 \theta(x)u(x, t)dx - cNBL(t) \quad (11)$$

where the integral expresses the outflux of granulocytes into the blood and c is the rate of disappearance from the blood - in the steady state obtainable from the value of the observed half-life of blood granulocytes. The function $\theta(x)$ may be the one defined in (10). To include the possibility that also circulating granulocytes participate in G-CSF elimination and thereby to the feedback effect, the extended system may allow for NBL to be included in the total effective neutrophil count z in the total system description:

$$z(t) = NBL(t) + \int_0^1 w(x)u(x, t)dx$$

This model may be used to give model descriptions of blood granulocyte engraftment in clinical situations such as high-dose therapy with stem cell support. The model described above is capable of giving good model estimates of the increasing blood neutrophil count during engraftment, as shown by the example in Figure 2A. Here, it is seen that the model estimate of blood neutrophil count (solid line) yields a constant output once the system has reached a steady state.

3. Stability analysis

3.1. Simplified system of equations

As a first approximation to the more complicated system, we will assume the following simplifications:

The net proliferation rate α is assumed to be composed of a constant term α_0 , a linear term including $y(t)$ which models the cytokine(G-CSF) influence on the net proliferation (including possible apoptosis), and a term θ to model the rate of mobilization to blood from the bone marrow, here assumed constant over the maturity scale as a first approximation, i.e.,

$$\alpha(y) = \alpha_0(a + by) - \theta. \quad (12)$$

With reference to the biological situation, the steady state is assumed to be characterized by a positive value of α . Hence, parameter values must be chosen accordingly.

In the more realistic approach, α_0 as well as θ are functions of x , $\theta(x)$ being confined to the last part of the maturity (x) scale. In this approach, due to zero values of α_0 and positive θ values at the end of the maturity scale, $\alpha(x, y)$ will assume negative values in a short x interval.

a, b are constant, positive parameters governing the sensitivity of α relative to changes in G-CSF concentration (the mitotic responsiveness).

The maturation rate β is here assumed to be a constant.

The function $z(t)$ is taken to be the total granulocyte count in the bone marrow, i.e., we assume $w(x)$ in (4) to be constant and equal to 1:

$$z(t) = \int_0^1 u(x, t) dx.$$

The function $f(y, z)$ in (3) describes the elimination rate of G-CSF due to neutrophils. This function was estimated as in (5):

$$f(y, z) = k_1 y + k_2 z [1 - e^{-\frac{k_3 y}{z+p}}], \quad (13)$$

where the last term includes elimination of G-CSF by neutrophil receptors. This is a decreasing function of the cell number z . k_1, k_2, k_3, p are constant, positive parameters.

When $z \approx 0$, (13) expresses a model with first order elimination. Hence, k_1 could be estimated by means of measurements of G-CSF half-life after exogenous doses of G-CSF at neutropenia ($z \approx 0$). When $z \neq 0$, the second term in (13) models a G-CSF receptor elimination with saturation at large values of z . In the latter

case, the limiting value of $f(y, z)$ can be shown to be $(k_1 + k_2k_3)y$. The parameters k_2, k_3, p could be estimated by comparing the resulting G-CSF half-life from the model with actual half-lives recorded for varying values of the cell count z . In doing so, (13) could be approximated by the estimate

$$f(y, z) = k_1y + k_2z[1 - e^{-\frac{k_3y}{z+p}}] \approx k_1y + k_2k_3\frac{z}{z+p}y$$

by omitting higher order terms in the Taylor series for the exponential. Because of the orders of magnitude of k_2, k_3 , the error introduced is of a negligible relative order of $9.0 \cdot 10^{-15}$. This approximation facilitates later calculations.

In this way, (3) can be represented by the equation

$$y_t = y_{PROD} - g(z)y(t) \quad (14)$$

where

$$g(z) = k_1 + k_2\frac{z}{z+p} \quad (15)$$

and where the new positive constant k_2 has been substituted for the former product k_2k_3 for convenience.

As a conclusion, the model (1)–(8) is transformed into the following set of simplified equations:

$$u_t + \beta u_x = \alpha u, \quad (16)$$

$$y_t = y_{PROD} - g(z)y(t), \quad (17)$$

with initial and boundary conditions

$$u(x, 0) = u_0(x), \quad (18)$$

$$\beta[0, y(t)]u(0, t) = Q(t) = \text{constant}, \quad (19)$$

$$y(0) = y_0, \quad (20)$$

and with the constitutive relations

$$\alpha = \alpha_0(a + by) - \theta = \alpha(y), \quad (21)$$

$$z(t) = \int_0^1 u(x, t)dx. \quad (22)$$

The initial condition (18) refers to a distribution of cell density $u_0(x)$ given as input to the model. This function may be calculated on the basis of an assumed function for the proliferation rate $\alpha(x)$ for neutrophil progenitors and precursors, as was done in [41]. As a first approximation, the function $u_0(x)$ may be taken as a constant.

Because of the nonlinearity of the function $g(z)$ included in (17) and the by term in (21), this system should be classified as nonlinear.

3.2. Characterization of a steady state

The system (16)–(20) may be linearized with respect to a steady state given by the conditions

$$u_t = 0, y_t = 0.$$

If the latter condition is inserted into (17), it is readily seen that the steady state value of y is given by

$$\bar{y} = \frac{y_{PROD}}{g(\bar{z})} \quad (23)$$

where \bar{z} is the steady state value of z .

The steady state condition leaves u as a function of x , in the following called $\bar{u}(x)$. (16) implies

$$\beta \bar{u}_x = \alpha(\bar{y}) \bar{u}$$

where $\alpha(\bar{y}) = \alpha_0(a + b\bar{y}) - \theta$.

This implies

$$\bar{u}(x) = u_0 e^{\alpha(\bar{y}) \frac{x}{\beta}} \quad (24)$$

and yields a steady state value of z given by

$$\bar{z} = \bar{z}(\bar{y}) = \int_0^1 \bar{u}(x) dx = \frac{u_0 \beta}{\alpha(\bar{y})} (e^{\frac{\alpha(\bar{y})}{\beta}} - 1). \quad (25)$$

According to (24), (25), \bar{u} and \bar{z} are explicit functions of \bar{y} .

It remains to show that the steady state given by the triple \bar{y} , \bar{z} , \bar{u} is unique.

Since \bar{z} is a function of \bar{y} by (25), it follows from (23) that

$$\bar{y} = \frac{y_{PROD}}{g(\bar{z}(\bar{y}))} = H(\bar{y}) \quad (26)$$

where the function $H(y)$ is an explicit function of y . It remains to show that $H(y)$ has a unique fixpoint, i.e., \bar{y} given by the condition (26).

The proliferation rate α may be assumed to be positive at steady state for all positive choices of β . This can always be achieved by proper choice of the parameters a , b , θ . Hence, the function $\bar{z}(y)$ given by (25) is a positive-valued function of \bar{y} . Since $\alpha(y)$ increases with y and the function $f(x) = \frac{1}{x}(e^x - 1)$ is strictly increasing (as can be seen from its Taylor series), it follows that $\bar{z}(y)$ given by (25) is strictly increasing with y . Furthermore, because of the continuity of the function $\alpha(y)$ given by (21) and hence the continuity of the function $\bar{z}(y)$ given by (25), we may conclude that the function $\bar{z}(y)$ is a continuous, positive, increasing function of y for all actual parameter values.

The limiting value \bar{z}_0 of $\bar{z}(y)$ as $y \rightarrow 0$ is

$$\bar{z}_0 = \lim_{y \rightarrow 0} \bar{z}(y) = \lim_{y \rightarrow 0} (u_0 \beta \frac{\alpha_y(y)}{\beta \alpha_y(y)} e^{\frac{\alpha(y)}{\beta}}) = u_0 e^{\frac{\alpha_0 a - \theta}{\beta}}.$$

The function $H(y)$ can be written

$$H(y) = \frac{y_{PROD}}{g(\bar{z}(y))} = \frac{y_{PROD}}{k_1 + k_2 \frac{\bar{z}(y)}{\bar{z}(y)+p}}.$$

The derivative of $H(y)$ must be negative for all actual parameter values. In fact, we have

$$H_y = -\frac{y_{PROD}}{g(\bar{z}(y))^2} g_z(\bar{z}) \bar{z}_y(y).$$

The function $g(\bar{z})$ is strictly increasing by (15) with p always positive. Furthermore, it was seen above that $\bar{z}(y)$ is also strictly increasing, hence H_y is always negative and $H(y)$ is descending from the limiting value $\frac{y_{PROD}}{g(\bar{z}_0)}$ to an asymptotic value

$$\lim_{y \rightarrow \infty} H(y) = \frac{y_{PROD}}{k_1 + k_2}.$$

This means that there exists a unique positive fixpoint \bar{y} .

3.3. Linearization, scaling, and characteristic equation

Linearization has been used as a standard procedure to gain insight into stability properties of non-linear systems like the ones describing, for instance, age-dependent population dynamics [8].

In the following, we deduce linearized equations from the system (16)–(20). Perturbated values of y , u , z relative to the steady state \bar{y} , \bar{u} , \bar{z} are given by

$$y = \bar{y} + Y, u = \bar{u} + U, z = \bar{z} + Z, \quad (27)$$

where the perturbations are $Y = Y(t)$, $U = U(x, t)$, $Z = Z(t)$. Linearization of (16),(17), omitting higher order terms in the perturbations, yields:

$$U_t + \beta U_x = A(x)Y + BU, \quad (28)$$

$$Y_t = CZ + DY, \quad (29)$$

$$Z(t) = \int_0^1 U(x, t) dx. \quad (30)$$

The initial and boundary values are given by

$$U(x, 0) = u(x, 0) - \bar{u}(x) = U_0(x), \quad (31)$$

$$U(0, t) = 0, \quad (32)$$

$$Y(0) = y_0 - \bar{y} = Y_0, \quad (33)$$

where (32) is a consequence of the fact that we assume no perturbation of the boundary data at $x = 0$.

The coefficients $A(x)$, B , C , D are given by

$$A(x) = \alpha_y(\bar{y})\bar{u}(x) = \alpha_0 b u_0 e^{\frac{\alpha(\bar{y})x}{\beta}} = A_0 e^{\frac{\alpha(\bar{y})x}{\beta}}, \quad (34)$$

$$B = \alpha(\bar{y}) = \alpha_0(a + b\bar{y}) - \theta, \quad (35)$$

$$C = -g_z(\bar{z})\bar{y}, \quad (36)$$

$$D = -g(\bar{z}). \quad (37)$$

We observe that the coefficients A , B , C , D are functions of β , since \bar{y} depends on β .

A reduction of the number of system parameters will simplify the interpretation of the conditions for stability. Hence, we rescale system (28)–(30) such that only three parameters, including β , are needed to describe the system. We define new variables by

$$t' = Bt, \quad x' = x, \quad \beta' = \frac{dx'}{dt'} = \frac{\beta}{B},$$

and

$$U' = \frac{C}{B}U, \quad Y' = Y.$$

Next, we introduce new positive-valued parameters q and r defined as:

$$q = -\frac{CA_0}{B^2}, \quad r = -\frac{D}{B}. \quad (38)$$

The scaled system we then obtain should be described in scaled variables U' , Y' , Z' , x' , t' , and β' . However, for notational simplicity, we will drop the primes here and in the following. We then arrive at the system

$$U_t + \beta U_x = -q e^{\frac{x}{\beta}} Y + U, \quad (39)$$

$$Y_t = Z - rY, \quad (40)$$

$$Z(t) = \int_0^1 U(x, t) dx, \quad (41)$$

$$U(x, 0) = \frac{C}{B}[u(x, 0) - \bar{u}(x)] = U_0(x), \quad (42)$$

$$U(0, t) = U_1(t) = 0, \quad (43)$$

$$Y(0) = y_0 - \bar{y} = Y_0. \quad (44)$$

The equation (39) may be solved by characteristics. According to the position on the time scale, there exist two different solution regimes. For large values of t ($t > \frac{1}{\beta}$), the solution may be written:

$$U(x, t) = -q e^{\frac{x}{\beta}} \int_{t-\frac{x}{\beta}}^t Y(s) ds.$$

This also implies a solution for Z by (41) given by

$$Z(t) = -q \int_0^1 e^{\frac{x}{\beta}} \int_{t-\frac{x}{\beta}}^t Y(s) ds dx.$$

This expression may be substituted in (40) to yield an integro-differential equation in $Y(t)$:

$$Y_t + rY = -q \int_0^1 e^{\frac{x}{\beta}} \int_{t-\frac{x}{\beta}}^t Y(s) ds dx. \quad (45)$$

By assuming a solution of this equation of the form

$$Y(t) = \tilde{Y} e^{\lambda t}$$

with $\lambda \neq 0$, (45) implies a characteristic equation in λ :

$$\lambda + r = -q\beta \left(\frac{e^{\frac{1}{\beta}} - 1}{\lambda} - \frac{e^{\frac{1-\lambda}{\beta}} - 1}{\lambda(1-\lambda)} \right). \quad (46)$$

This equation, valid for $\lambda \neq 0, 1$ and for $t > \frac{1}{\beta}$, will be used in the following to discuss potential stability changes as the maturation rate β changes values. It is seen by substitution that the values 0 or 1 for λ do not represent valid solutions.

For the case referring to the physiological situation, coefficients r, q in (46) must be considered continuous functions of β because A, B, C , and D are functions of the original maturation rate β . In Appendix A, we deduce lower and upper limits for the values of coefficients A, B, C , and D with the consequent lower and upper limits for r and q . Stability properties for the system will be discussed for the case with constant values of r and q as well for the case with r, q considered functions of β .

3.4. Appearance of engraftment curves

Figure 5 shows three examples of outputs $z(t)$ from the system (16)–(20) with slightly differing values of β : $\frac{1}{1281} h^{-1}$, $\frac{1}{1423} h^{-1}$, $\frac{1}{1601} h^{-1}$. In all cases, the constant initial and boundary value of $u(x, t)$ was chosen to be $1.5 \cdot 10^5$ c/kg bw. The figure suggests in each case the existence of an initial regime characterized by an exponentially increasing output as $t < \frac{1}{\beta}$. For larger values of t , the system appears to approach a stable situation.

3.5. Definition of stability

As an operative definition of stability, the following is adopted: The steady state solution (\bar{u}, \bar{y}) of the system (16)–(20) is stable when the L^1 norm of the solution $|U(x, t)|$ of the linearized system (28),(29),(30), $\int_0^1 |U(x, t)| dx$, as well as the absolute value of $Y(t)$ tend to zero when $t \rightarrow \infty$, for arbitrary initial conditions.

In addition, we assume that the solutions of the systems (16)–(20) and (39)–(44) are C^1 functions, implying that $u(x, t)$, $y(t)$, $U(x, t)$, $Y(t)$ and their first derivatives are continuous functions of x and t (see Appendix B).

3.6. Stability for large values of β

It will be shown that the linearized, simplified system (39)-(44) is stable for all choices of parameters as the maturation rate β is large enough, the precise meaning of this being that the coefficient q is smaller than a specified strictly increasing function of β . As a consequence, the simplified system (16)-(20) is stable as β grows without bounds, for fixed values of q and r .

To this end, we apply an energy argument (Appendix B) to show that with parameters r , q fixed and β large enough, we have:

$$\begin{aligned} \lim_{t \rightarrow \infty} \int_0^1 U^2(x, t) dx &= 0, \\ \lim_{t \rightarrow \infty} Y^2(t) &= 0. \end{aligned}$$

Since the L^2 norm $\int_0^1 U^2(x, t) dx$ bounds the L^1 norm, this will imply stability as defined above (3.5).

The stability condition referred to above as “ β large enough” can be written

$$q < \frac{2r}{\beta \sqrt{(1 - e^{-\frac{2}{\beta}})(e^{\frac{4}{\beta}} - 1)}}. \quad (47)$$

The argument given in Appendix B can be extended to the situation where coefficients r , q are functions of β as given by their dependence on the original coefficients A_0 , B , C , and D in (38). This is due to the boundedness of r and q between positive limits as shown in Appendix A. With β chosen large enough, the condition (47) can always be met as long as r and q are bounded, since the right-hand side expression above represents a strictly increasing function of β .

Figure 6 shows the graph of the expression on the right-hand side of the condition (47) as a function of β (referred to as $\sigma_r(\beta)$), plotted here with the choice $r = 1$.

3.7. Transitions between stable and unstable states

It has been shown that the system (39)-(44) is stable for any given parameter values as long as the maturation rate β is chosen large enough. Here, we will show in a semi-analytical way that the system may pass through regimes of instability and stability, depending on the choice of β and the remaining parameters. To this end, consider the characteristic equation (46) where the maturation time T has been substituted for $\frac{1}{\beta}$ for convenience:

$$\lambda + r = G(\lambda, T) \quad (48)$$

where

$$G(\lambda, T) = -\frac{q}{T} \left(\frac{e^T - 1}{\lambda} - \frac{e^{(1-\lambda)T} - 1}{\lambda(1-\lambda)} \right). \quad (49)$$

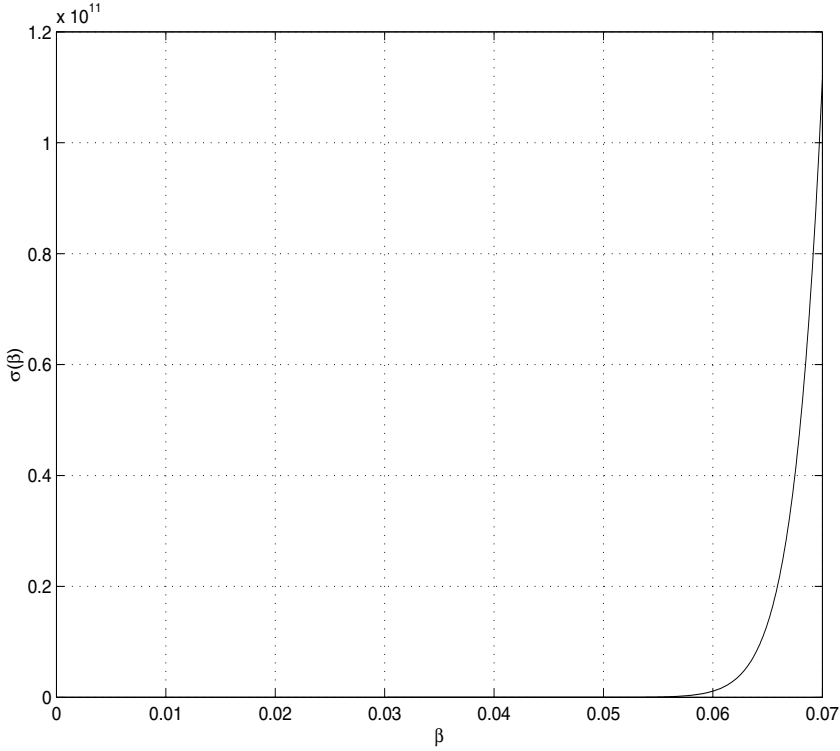


Fig. 6. Graph of the function $\sigma_r(\beta)$ given in (74), (the right-hand side of (47)), playing a role in the conditions for system stability with given values of parameters q , r , and β (Appendix B).

As shown in Appendix B, the system is stable as $\beta \rightarrow \infty$, or $T \rightarrow 0$. Assume that a transition between a stable and an unstable state occurs for a pure imaginary eigenvalue $\lambda = i\eta$, where $i^2 = -1$ and η is real. Furthermore, a necessary condition for a transition to instability must be that the derivative $\frac{d}{dT}(Re\lambda)$ be positive at the point of transition. This will ensure a transition from negative to positive values of the real part of λ and, hence, a transition to an unstable regime.

After substituting $\lambda = i\eta$ into (48), we get the two following equations for the real and imaginary part of the equation, respectively:

$$s \frac{e^T [\eta \cos(\eta T) - \sin(\eta T)] - \eta}{\eta T (\eta^2 + 1)} = 1, \quad (50)$$

$$q \frac{e^T [\eta^2 + 1 - \eta \sin(\eta T) - \cos(\eta T)] - \eta^2}{\eta T (\eta^2 + 1)} = \eta, \quad (51)$$

where the positive parameter s has been substituted for $\frac{q}{r}$.

These are nonlinear equations in η which must be satisfied for a given T (or β) to give a transition between stable and unstable states. Depending on the parameters, the equations may have no solutions for any finite positive T , or a number

of solutions. Numerical solutions given as values of (T, η) satisfying (50),(51) were obtained by applying the MATLAB minimizing procedure *fminsearch*, an unconstrained nonlinear optimization procedure designed to minimize a real-valued function of $x \in \mathcal{R}^n$ and using the Nelder-Mead algorithm [29]. The procedure was applied to find local minima $(T^*, \eta^*) = (\frac{1}{\beta^*}, \eta^*)$ for the sum of the relative squared differences between the right-hand and left-hand sides of (50),(51).

In Figure 7, a solution at $T = 4.9028$ ($\beta = 0.2040$) is depicted by means of the graphs of the left-hand and right-hand side of (50)–(51) on figure A and B, respectively, with points corresponding to a solution marked with a circle. Figures 7 C and D show the situation for the smaller value $T = 2.0000$ ($\beta = 0.5000$), where no solution is obtained because of the failing solution for the real parts (Figure C). Figures 7 A and B correspond to a transition to an unstable state (see comments to Figure 8), Figures 7 C and D correspond to a stable state.

If we assume that λ depends smoothly on T , two conclusions can be drawn from inspection of (50):

- 1) A necessary condition for a transition to instability is that the left-hand side expression of (50) have a global maximum value which equals or exceeds 1.
- 2) The first possible stability change as T increases from zero may occur as the global maximum value of the left-hand side of (50) assumes the value 1. This may occur as a result of increasing T , s , or both.

We turn now to the sign of $\frac{d}{dT}(Re\lambda)$, determining the nature of the stability change given by the solution of (50),(51). Implicit derivation of (48) gives:

$$\frac{d\lambda}{dT} - G_\lambda(\lambda, T) \frac{d\lambda}{dT} - G_T(\lambda, T) = 0,$$

which again implies

$$\frac{d}{dT}(Re\lambda) = Re\left[\frac{G_T(\lambda, T)}{1 - G_\lambda(\lambda, T)}\right] = \frac{(1 - ReG_\lambda)ReG_T - ImG_T ImG_\lambda}{(1 - ReG_\lambda)^2 + (ImG_\lambda)^2}.$$

This means that the sign of $\frac{d}{dT}(Re\lambda)$ is determined by the parameter ω defined by

$$\omega = (1 - ReG_\lambda)ReG_T - ImG_T ImG_\lambda. \quad (52)$$

As a further condition, it must be shown that a potential stability change given by $Re(\lambda) = 0$ and $\frac{d}{dT}[Re(\lambda)] \neq 0$ is a real change; i.e., that $Re(\lambda)$ changes continuously as T passes the value for which $Re(\lambda) = 0$. To this end, consider the characteristic equation (48), substitute $\lambda = \kappa + i\eta$ and write (48) in the general form

$$F(T, \kappa, \eta) = \begin{bmatrix} f_1(T, \kappa, \eta) \\ f_2(T, \kappa, \eta) \end{bmatrix} = \begin{bmatrix} Re(\lambda + r - G(\lambda, T)) \\ Im(\lambda + r - G(\lambda, T)) \end{bmatrix} = \begin{bmatrix} 0 \\ 0 \end{bmatrix}, \quad (53)$$

where f_1, f_2 are functions of T, κ, η defined as the real and imaginary part of $\lambda + r - G(\lambda, T)$, respectively, as defined in (48),(49).

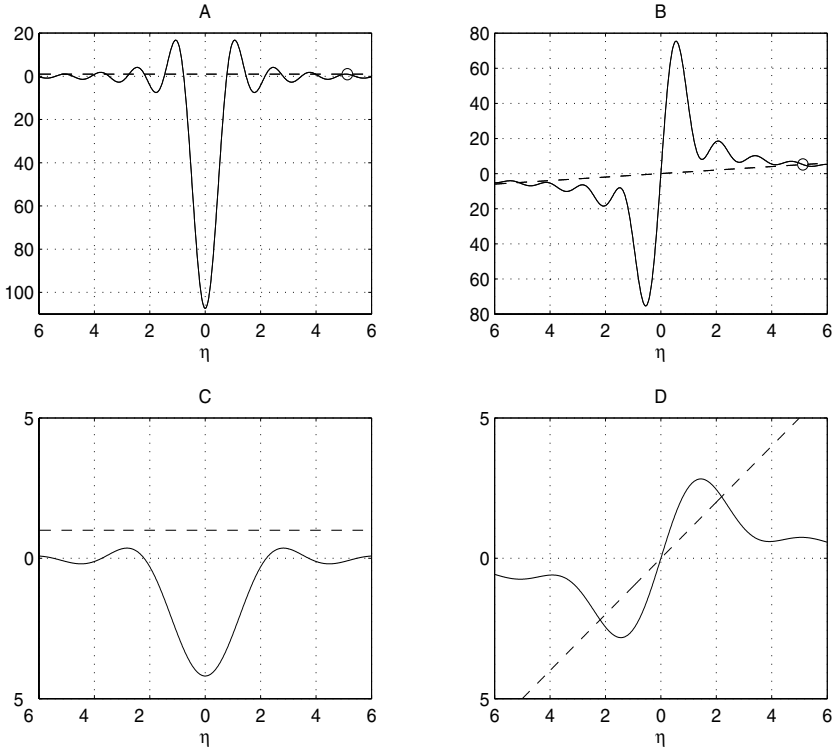


Fig. 7. A): Solid line: The left-hand side of (50) with a pure imaginary $\lambda = i\eta$ corresponding to a transition between a stable and an unstable state of system (39)–(44), plotted as a function of η . The value of T is 4.9028 at $r = 1, q = 1, s = 1$, corresponding to a transition from a stable to an unstable state. Points corresponding to a solution of (50)–(51) are marked with a circle. Dotted line: The right-hand side of (50) as a function of η , having the constant value 1.

B): Solid line: The left-hand side of (51) with a pure imaginary $\lambda = i\eta, T$ and remaining parameters as in panel A. Dotted line: The right-hand side of (51) as a function of η (the identity function).

C): Plot analogous to Figure A. The value of T is now reduced to 2.0000 at $r = 1, q = 1, s = 1$, corresponding to no solution of (50). This corresponds to a stable state.

D): Solid line: The left-hand side of (51) with a pure imaginary $\lambda = i\eta, T$ and remaining parameters as in panel C.

Referring to the general implicit function theorem [2], F is a C^1 function on a subset of \mathcal{R}^3 containing a solution triple of (53): (T_0, κ_0, η_0) where $\kappa_0 = 0$. If it can be shown that the Jacobian given by

$$J(T_0, \kappa_0, \eta_0) = \begin{vmatrix} \frac{\partial f_1}{\partial \kappa} & \frac{\partial f_1}{\partial \eta} \\ \frac{\partial f_2}{\partial \kappa} & \frac{\partial f_2}{\partial \eta} \end{vmatrix}_{(T_0, 0, \eta_0)} \quad (54)$$

is different from zero, then the function F is one-to-one in a neighborhood of $(T_0, 0, \eta_0)$, implying that $Re(\lambda) = \kappa$ must behave as a continuous function of T

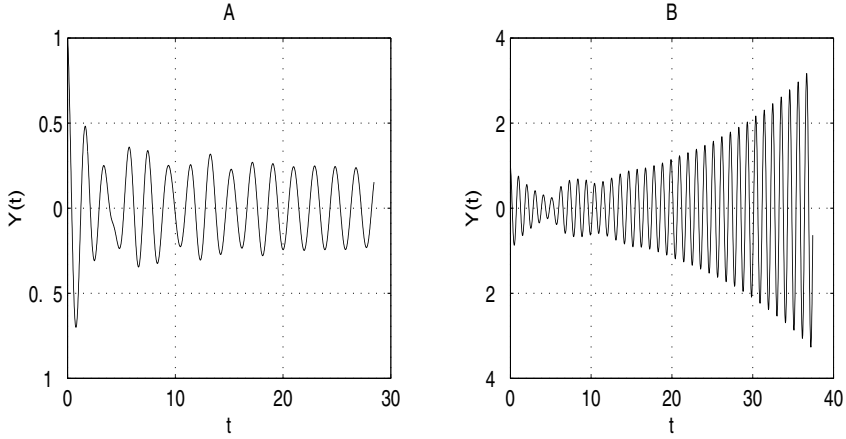


Fig. 8. A): Output $Y(t)$ from system (39)–(44) with $r = 1, q = 1, s = 1$ and $T = 4.0000$, illustrating stability for T smaller than the transition value 4.9028. B): Output $Y(t)$ from system (39)–(44) with $r = 1, q = 1, s = 1$ and $T = 5.2632$, illustrating instability for T greater than the transition value 4.9028.

Table 1. Results from numerical evaluations of transition points between stable and unstable states.

Case No	r	q	s	β^*	η^*	ω	J	Property
1	1	1	1	0.2040	5.1258	0.0574	48.9156	$Re(\lambda) \rightarrow pos.$
2	1	1	1	0.1214	21.3654	-0.0836	104.9095	$Re(\lambda) \rightarrow neg.$
3	1	10	10	0.7226	4.5399	0.0058	14.7772	$Re(\lambda) \rightarrow pos.$
4	1	10	10	0.4655	5.8505	-0.0178	19.7013	$Re(\lambda) \rightarrow neg.$

and hence change its sign at $(T_0, 0, \eta_0)$ if we have established that $\frac{d}{dT}[Re(\lambda)] \neq 0$ at the point where $\kappa = 0$.

In Table 1, numerical solutions η^* and $T^* = \frac{1}{\beta^*}$ of (50),(51) together with corresponding values of the parameter ω given by (52) are given. In addition, the Jacobian J given by (54) is presented for two choices of parameter values: $r = 1, q = 1, s = 1$, and $r = 1, q = 10, s = 10$. In all these examples, $J \neq 0$, while ω has different signs.

Case no.1 represents a transition to positive values of $Re(\lambda)$ as T increases from zero for the given values of r, q, s . Smaller values of T gave no solutions of (50), suggesting that this transition point represents the first possible transition to instability as T increases from zero (β decreasing from ∞). Figure 8 also suggests that this may be a point of transition to instability, showing the result of choosing T below (figure A, stable situation) and above (Figure B, unstable situation) the critical value found: $\frac{1}{\beta^*} = 4.9028$. The suggestion of a transition to instability is further supported by the positive value of ω while the Jacobian J is nonzero.

Case no.2 represents a transition to negative values of $Re(\lambda)$ due to the negativity of ω while the Jacobian J is nonzero. However, the system was still observed to be non-stable at higher values of T due to the persistent existence of an eigenvalue with positive real part.

Case no.3 represents a transition to $Re(\lambda) > 0$ for this particular choice of parameters. Again, it was seen numerically (not shown) in the same manner as with Figure 8 that this case may represent a transition to instability for this particular choice of parameters.

Case no.4 represents a new change of sign of $Re(\lambda)$ due to the negativity of ω , this time a change to negative values. With no other eigenvalues with positive real part, this corresponds to a transition to stability.

The following general statements may be made about system stability:

- T values increasing from zero may lead to unstable or stable regimes depending on T and the other parameters.
- Parameter values may be chosen to ensure stability for all values of T bounded between zero and a physiologically correct, chosen value. This will happen if (50) has no solution for any T inside that boundary, i.e., if s is chosen small enough to ensure that

$$s \frac{e^T [\eta \cos(\eta T) - \sin(\eta T)] - \eta}{\eta T (\eta^2 + 1)} < 1 \quad (55)$$

for any such values of T , any values of η . Since the system was shown to be stable for $T = 0$ ($\beta \rightarrow \infty$) and no transition to instability is possible because of (55), stability will follow.

- A necessary condition for system instability at a chosen T value is that the parameter s be large enough to ensure that

$$s \frac{e^T [\eta \cos(\eta T) - \sin(\eta T)] - \eta}{\eta T (\eta^2 + 1)} \geq 1 \quad (56)$$

for some $T = T^*$ in the interval between zero and the chosen T value and for some η . Then the system may potentially undergo a transition to instability for $T = T^*$, provided that (50),(51) is satisfied for $T = T^*$ and some value of η, q .

4. Discussion

4.1. Stability for physiologically correct values of β

For a given choice of parameters, it may be possible to show system stability by establishing (55) for all T between 0 and the T value actually chosen for the system. In other words, if the choice of parameter s can be shown to be sufficiently small to satisfy (55) for all $\eta \in \mathcal{R}$ and for all T in the given range, then the system can be said to be stable for the chosen T .

In fact, we can conclude more than this. The parameter s , being a function of coefficients A_0, B, C , and D , may be written as

$$s = \frac{q}{r} = \frac{CA_0}{BD} = \frac{g_z(\bar{z}) \alpha_y(\bar{y})}{g(\bar{z}) \alpha(\bar{y})} \bar{y}$$

by using the definitions of A_0 , B , C , and D given in (34)–(37). From this expression, we can conclude: By given normal physiological values of the endogenous cytokine level \bar{y} and the output cellularity \bar{z} at steady state, there are certain upper limits for the relative mitotic responsiveness defined as $\frac{\alpha_y(\bar{y})}{\alpha(\bar{y})}$ and the “relative cytokine elimination responsiveness” $\frac{g_s(\bar{z})}{g(\bar{z})}$ which must not be exceeded in order to ensure stability at a physiologically correct β . This follows from the sufficient condition for stability that s be small enough to satisfy (55) for all T between 0 and the chosen T value for the system. But s as well as the expression in T , η in (55) depend on T (β), since \bar{y} , \bar{z} depend on β by (23),(25). Hence, there is no simple chain of implications between the choice of β and the conclusions regarding stability. We show here, however, that with a choice of parameters α_0 , a , b , θ , u_0 , k_1 , k_2 , y_0 , y_{PROD} , and p which ensures physiologically correct values of \bar{y} and \bar{z} , the system will keep stable as T increases from zero to a value corresponding to the chosen, physiologically correct value of β .

Referring to (21), the choice of parameters a and b decides the proliferation rate at a given cytokine level y . Given the values of the other parameters, the choice $a = 3.0$, $b = 0.001$ gives as output values for the steady state: $\bar{z} = 2 \cdot 10^8$ c/kg bw, $\bar{y} = 350$ pg/ml (endogenous G-CSF) which may be considered realistic values for a semi-neutropenic steady state. For a realistic maturation time T , we adopt $T = 1281h$ as the maturation time from the early LTC-IC progenitor stage to the most mature PMN granulocyte stage, hence $\beta = \frac{1}{1281h}$ [41].

Secondly, we re-substitute the *real* maturation time T into (50) (remembering the original scaling of the time axis given by $t' = Bt$) and observe that s is a function of β , and hence a function of T due to $s = \frac{q}{r}$, (38),(34)–(37),(23),(25). Hence, (50) becomes

$$s(T) \frac{e^{BT} [\eta \cos(\eta BT) - \sin(\eta BT)] - \eta}{\eta BT (\eta^2 + 1)} = 1.$$

Since this is a necessary condition for a transition to instability, we will show that the function given by

$$\xi(\eta, B(T), T) = s(T) \frac{e^{BT} [\eta \cos(\eta BT) - \sin(\eta BT)] - \eta}{\eta BT (\eta^2 + 1)}$$

is smaller than 1 for T inside the range $< 0, 1281h >$ for the parameter values chosen and for all $\eta \neq 0$, i.e. that (55) is satisfied.

Consider the alternative expression

$$\eta \cos(\eta BT) - \sin(\eta BT) = \sqrt{\eta^2 + 1} \cos(\eta BT + \phi)$$

yielding the following estimate for positive η (omitting negative η because of symmetry):

$$\xi(\eta, B(T), T) \leq s(T) \frac{e^{BT} \cos(\eta BT + \phi)}{\eta BT \sqrt{\eta^2 + 1}}. \quad (57)$$

Here, ϕ is an angle in the interval $< 0, \frac{\pi}{2} >$ given by

$$\phi = \arctan\left(\frac{1}{\eta}\right).$$

The first maximum of the expression $\cos(\eta BT + \phi)$ with positive η occurs at $\eta BT + \phi = 2\pi$, thus implying that η is confined to the interval

$$\eta\epsilon < \frac{3\pi}{2BT}, \frac{2\pi}{BT} > \quad (58)$$

at the first maximum of $\cos(\eta BT + \phi)$ for a given value of T .

Since the function of η at given T given by

$$h(\eta) = \frac{\cos(\eta BT + \phi)}{\eta BT \sqrt{\eta^2 + 1}}$$

is one with a strictly decreasing amplitude, (57) with (58) yield the estimate

$$\xi(\eta, B(T), T) \leq s(T) \frac{e^{BT}}{\frac{3\pi}{2} \sqrt{\left(\frac{3\pi}{2BT}\right)^2 + 1}} \equiv \psi(T). \quad (59)$$

A numerical evaluation of the function $\psi(T)$ defined by the right-hand side of the inequality above for the parameter values chosen is seen in Figure 9 and compared with the constant 1. The figure shows that the value of $\psi(T)$ is smaller than 1 for all T in the range from 0 to 1281 h, thus suggesting stability since the sufficient condition for stability (55) is apparently satisfied. The figure also shows the similar result for the parameter b equal to 0.01, thus increasing the relative mitotic responsiveness as defined earlier but still indicating stability for this b value.

The system discussed above did not include an x dependent α , as was the case in the original system. In that case, the linearized system (28)–(30) will now include an x dependent coefficient $B = B(x)$ as well as $A(x)$. This makes it difficult to scale the system in the same manner as was done to obtain (39)–(44).

Nevertheless, the argument used to show stability as β grows without bounds may still be applied to the system (28)–(30). By noting that coefficients $A(x)$ and $B(x)$ must be bounded above by a common constant as β increases, one may obtain an estimate for $E_t(t)$ in the same manner as was shown by (65) in Appendix B. This means that a slight modification of the argument shows that the system is still stable as $\beta \rightarrow \infty$ even with α dependent on x .

The extension of the characteristic equation (46) for this case will involve integrals containing $A(x)$ and $B(x)$ not generally solvable by elementary functions. This means that extensions of (50),(51) obtained by substituting $\lambda = i\eta$ into (46) to explore conditions for transitions to instability can only be analyzed by numerical means. However, by following the same guidelines as traced out here, it may be shown numerically that for most realistic model cases, the system will still be stable for physiologically correct values of β and the other parameters. Furthermore, it may be shown that with the values of $\alpha(x)$ for a given y never exceeding an α value shown by the present analysis to yield stability, the system is still stable even when α depends on x .

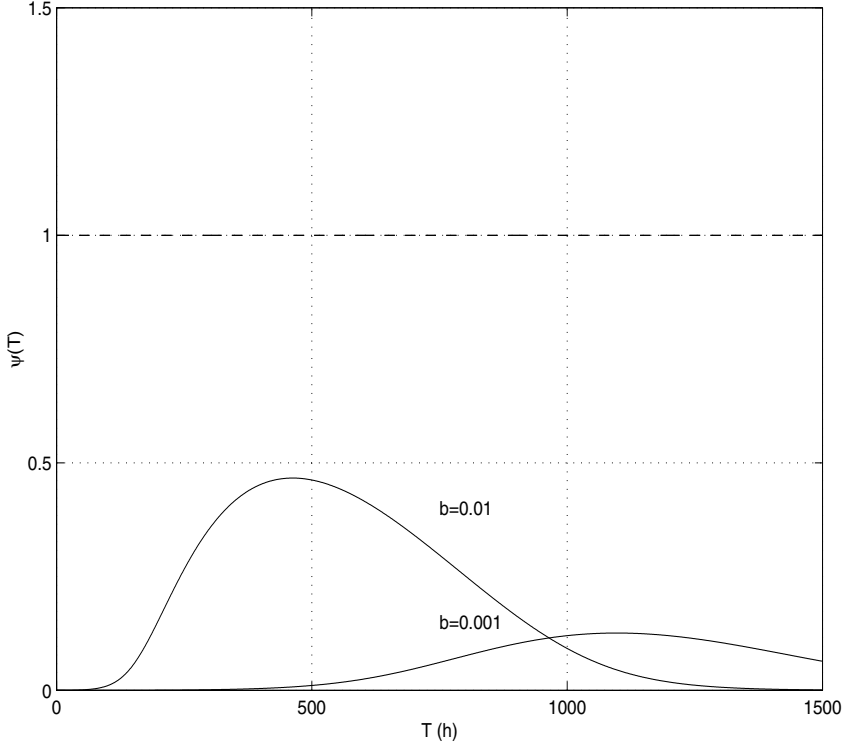


Fig. 9. Solid lines: Graph of the function $\psi(T)$ defined in (59) as an upper estimate for $\xi(y, B(T), T)$ in (57). Function values are compared to the constant 1, thus indicating stability since (50) is not satisfied for any T values from zero up to the value of 1281 h adopted as physiologically correct. Shown are graphs of $\psi(T)$ for two values of parameter b .

4.2. Stable limit cycles

The observed picture of the original system output may be modified in the sense that the system may be brought to enter a state of cyclic variations of the output with constant amplitude and frequency. For the present model, it may be demonstrated that the choice of values of parameters a , b regulating the sensitivity of α to changes of cytokine levels y (21) has direct consequences for the nature of the system output. In Figure 10 A (corresponding to the stable situation), the choice was $a = 1.27$, $b = 2.6 \cdot 10^{-4}$, while Figure 10 B shows the result of choosing $a = 1.0$, $b = 1.8 \cdot 10^{-3}$. Referring to (21), this means a much higher sensitivity for changes of the G-CSF level, while the amplification of α at the steady state is diminished as indicated by a . It is seen that while the steady state output level is much diminished, the system has entered a state of oscillations of the output with constant amplitude and frequency, much resembling states like cyclic neutropenia where the blood granulocyte count fluctuates with a period of about 20 days [35]. Furthermore, with parameter a still equal to 1.0 while b is reduced to $8.0 \cdot 10^{-4}$, the

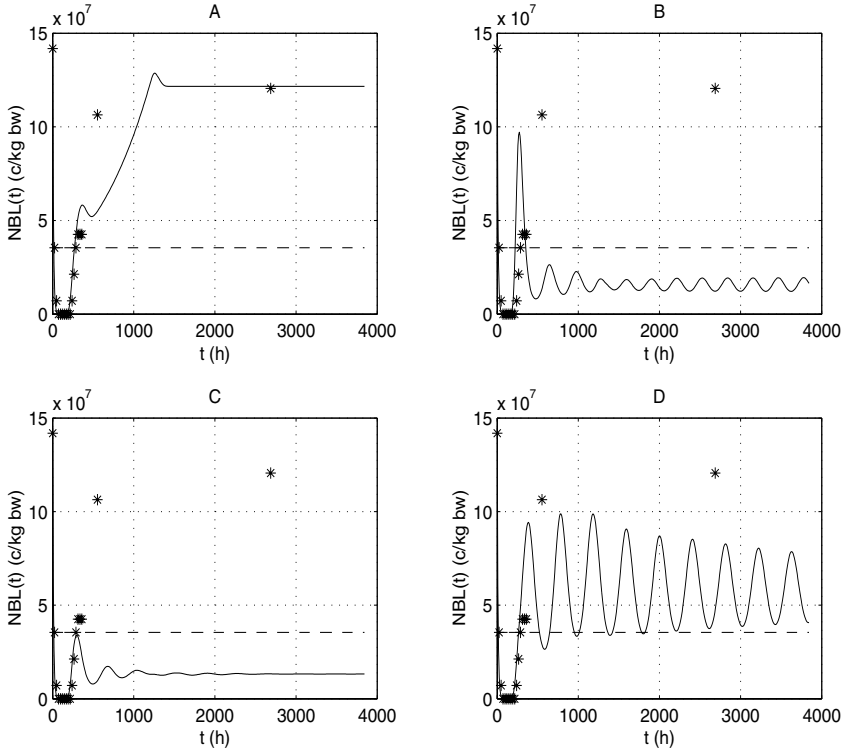


Fig. 10. A): Output from the system (16)–(20) extended with (11) and α, θ given by (9),(10): The solid line shows the modeled blood granulocyte count $NBL(t)$ as function of time t after reinfusion of an autologously derived, enriched CD34+ product as described in section 3.2. Stars: Observed patient data from one selected patient. Values of α amplification parameters are $a = 1.27, b = 2.6 \cdot 10^{-4}$. B): Output from the same system with parameter values altered to $a = 1.0, b = 1.8 \cdot 10^{-3}$. C): Output from the same system with parameter values altered to $a = 1.0, b = 8.0 \cdot 10^{-4}$. D): Output from the same system with parameter values as in Panel C, but with argument z to function $g(z)$ in (15) set equal to $NBL(t) + 0.10 \cdot NB(t)$. $NBL(t)$ and $NB(t)$ are total blood and bone marrow granulocyte count, respectively.

system enters again a state with a constant steady state output as shown in Figure 10 C. This suggests that the relative mitotic responsiveness for a given x given by

$$\frac{\alpha_y(\bar{y})}{\alpha(\bar{y})} = \frac{\alpha_0(x)b}{\alpha_0(x)(a + b\bar{y}) - \theta(x)}$$

may be a crucial factor for the system transition between a constant and an oscillating steady state output. According to this, for a given value of the parameter a , there are certain limits to the b value which must not be exceeded to ensure system operation without oscillations. However, the observed oscillating behavior is still stable in the sense adopted here since no amplification of the amplitude takes place as time increases.

For the simplified system where α as well as θ were constant in x , the same tendencies to oscillating behavior could be observed under the same condition as noted here. However, in these cases, oscillations were invariably subject to damping in a way that the system output quickly settled on a constant level. Consequently, the undamped cycling behavior must be said to be a feature belonging to the original model.

A second feature of the original model deserves a comment. In the case of a weak α amplification in the steady state (small value of a) as shown in Figures 10 B and C, the system is extremely sensitive to changes in the feedback signal. This means changes in the argument z of the function $g(z)$ (15), biologically explainable as the effective number of cell receptors participating in the elimination of the cytokine (G-CSF). Normally, the input z was taken to be the total bone marrow granulocyte cellularity, possibly with the addition of the blood neutrophil count NBL . However, system response may be altered by assuming that only a certain part of the bone marrow granulocytes or precursors may contribute to elimination of the cytokine. Figure 10 D shows the result of assuming the same parameter values as in Figure 10 C, but where z is effectively equal to NBL plus only 10 percent of the total bone marrow granulocyte count. It is seen that violent oscillations occur, even if they are subject to effective damping as time increases.

The investigations shown suggest that with abnormal values of the relative mitotic responsiveness, the system is especially sensitive to abnormalities of the cells' elimination of cytokine. No such effect was observed with normal values of the mitotic responsiveness. Further investigations will be needed to clarify this important point.

4.3. Properties of the simplified and the original system

The simplified PDE system shows the following features:

- Instability for all parameter values as $\beta \rightarrow 0$
- Stability for given finite values of β when parameter values satisfy certain conditions
- Stability for all parameter values as β grows without bounds
- For certain finite β values, choices of parameters are possible which bring the system into unstable regimes. These choices correspond to an increased relative mitotic responsiveness or cytokine elimination responsiveness.
- For physiologically correct values of β and other parameters, a transition to instability in the sense that $Re(\lambda) = 0$ may be impossible.

For the original system involving α , θ dependent on x and with a blood compartment added, the following was observed:

- The system shares the properties of the simplified system as $\beta \rightarrow \infty$ and as β approaches physiologically correct values.
- Choices of parameter values are possible which imply transition to a cyclic state. These choices correspond to a diminished steady state amplification of proliferation combined with a relatively high mitotic responsiveness. Amplitudes may be amplified by assuming a reduction of the effective number of cells participating in cytokine elimination.

4.4. Results from other models

The stability of the present simplified system was shown to depend on the maturation rate β in the way that certain values of β may induce system instability. So far, this is consistent with results from more general delay models as described by MacDonald [21]. Indeed, it is possible to show the equivalence between the present model and a system including time delay due to the finite maturation time through the system.

Alternative models showing state transitions as a consequence of increased maturation time are described in [22], [23], [24]. However, these authors treat stable limit cycles as cases of instability, in contrast to what is done here. Mackey et al's granulopoiesis model [24] equipped with a feedback function with an absolute maximum for intermediate values of the delayed granulocyte count shows a rich variation of unstable states: With increasing time delay, periodic solutions turn into a sequence of period-doubling bifurcations followed by a chaotic behavior. We are unaware of any observations of chaotic behavior of real blood neutrophil data. Also, no such chaotic behavior has been observed in the present model, with the exception of apparent chaotic behavior as a consequence of a too large time step in the numerical algorithm.

It is important to realize that the present model, equipped with parameter values corresponding to normal granulopoiesis, shows a remarkable stability. A way to provoke this stability is to change the characteristics of the mitotic responsiveness, thus opening for transitions to cyclic states.

One may pose the question of how the observations on cyclic states fits in with physiological observations. According to Wright et al [40] and Hammond et al [9], granulocyte-macrophage progenitor cells (CFU-GM) taken from patients with cyclic neutropenia demonstrated abnormal *in vitro* proliferative responses when subjected to purified, recombinant human granulocyte-macrophage colony-stimulating factor (rhGM-CSF). Some of these abnormalities included a right shift of the dose-response curves and a consequent significant great increase in rhGM-CSF concentrations that induced half-maximal responses, but also, especially for the growth of 7 day CFU-GM, a significant difference in the shape of the dose-response curve showing an enlarged mitotic responsiveness for higher molar rhGM-CSF concentrations. This result, pointing at a link between cyclic states and mitotic responsiveness, is in accordance with general properties of the present model modified with x -dependent α and θ .

Also, this result seems to be consistent with the results from the models by Schmitz et al [30], who found that a change of shape of the response function (i.e., the mitotic responsiveness) in accordance with the results of Wright [40] implied a transition to cyclic states of the system.

A somewhat parallel property was observed by Mackey et al [22], [23], [24] concerning their model of erythropoiesis. In this model, an increase in the maximal slope of the feedback function implies an onset of limit cycle behavior of the output number of erythrocytes. This is a parallel to the concept of mitotic responsiveness, even if no cytokine is included in Mackey et al's model as a link between cell count and the production rate function.

It was observed with the present original model that with a certain choice of parameters, the system may be brought into a state of more violent oscillations by reducing the amount of cells participating in cytokine elimination. Mathematically, this behavior is partly explainable as a result of a generally diminished value of the feedback signal $z(t)$. With $z(t)$ having decreased values, $y(t)$ will consequently increase because of (14). This effect will be equivalent to an increased value of the parameter b (21), leading to a possible transition to cyclic states as seen in Figure 10 B.

The feedback signal rests on the ability of more or less mature cells to eliminate the cytokine in question and thereby to affect the general cytokine level in the system. This ability of the cells depends again on certain receptors on the cell surface, receptors which may be subject to defects of genetic or acquired origin. One possible explanation of congenital cyclic neutropenia, for instance, may be a partly defective set of receptors for G-CSF or other cytokines of vital importance for neutrophil growth. Furthermore, such a defect may be maturity dependent, thus possibly leading to a feedback signal with properties as seen in the present model.

In alternative models, cyclic states are explained as a consequence of altered mitotic responsiveness [23], [24], [30], by a reduced mobilization rate relative to the production rate [35], by a prolonged maturation time [24], [35], or by a diminished variance of cell transit times through the system [30].

Recent modeling results by Haurie et al [12], [13], [14], [15] support the hypothesis that the main origin of the cyclic hematological diseases may be found in cyclic variations of cellularity at the stem cell level, taken to be due to some defect in the autoregulation of totipotent stem cells at a level prior to differentiation into the various cell lineages. The observation that cyclic neutropenia most often is seen together with cyclic variations in platelets, lymphocytes, and erythrocytes may support this view [11], [12]. Model studies [15] indicate that the observed variations in blood neutrophil cellularity in patients with cyclic neutropenia may be predicted by assuming a sinusoidal variation of stem cell cellularity filtered through a globally stable nonlinear peripheral control loop controlled by a feedback action through G-CSF. However, a defective autoregulation of a stem cell compartment separated from a peripheral regulatory loop controlled by G-CSF may not be the only possible origin of cyclic neutropenia. As suggested by the numerical investigations of the present model, the granulopoietic system may be brought into regions of stable limit cycles by, for instance, altering the maturity distribution of neutrophils participating in G-CSF elimination.

Extended investigations with the original model under extreme conditions like stem cell transplant and G-CSF treatment after complete neutropenia showed no tendency to instability. This is consistent with clinical observations of circulating neutrophils in patients having undergone high dose chemotherapy with stem cell support. As shown with the simplified model, stability is persistent as long as the maturation rate has physiologically plausible values and as long as there is a wide distribution of maturities for the neutrophils taking part in G-CSF elimination, as normally may be the case.

More precise conditions for the original model to switch into cyclic or even unstable states deserves a closer mathematical investigation and may be a suggestion for further work in the field.

Acknowledgements. This work has received financial support from the Norwegian Cancer Society.

5. Appendix A

It will be shown that the original coefficients A, B, C, D given by (34)–(37) behave as continuous functions of β with definite upper and lower limits, provided the other parameters are kept fixed.

Consider first the linearized equation system (28)–(30), and consider the limiting cases $\beta \rightarrow \infty$ and $\beta \rightarrow 0$.

Firstly, we note that \bar{y} will keep bounded between finite values, since (26) and the definition of g in (14) give:

$$\frac{y_{PROD}}{k_1 + k_2} \leq \bar{y} \leq \frac{y_{PROD}}{k_1}. \quad (60)$$

Furthermore, it can be seen from the expression for \bar{z} given by (25) that

$$\bar{z} = \frac{u_0 \beta}{\alpha(\bar{y})} (e^{\frac{\alpha(\bar{y})}{\beta}} - 1).$$

This implies that

$$\lim_{\beta \rightarrow \infty} \bar{z} = u_0.$$

In other words, as $\beta \rightarrow \infty$, there will be no effective proliferation through the system.

For the second case, when β approaches zero, it can be shown that \bar{z} will increase without bounds. To see this, note again that \bar{y} is bounded between two finite values as given in (60). With \bar{y} confined between these two values, it can be seen that \bar{z} given by (25):

$$\bar{z} = \frac{u_0 \beta}{\alpha(\bar{y})} (e^{\frac{\alpha(\bar{y})}{\beta}} - 1)$$

will increase without bounds as $\beta \rightarrow 0$, hence

$$\lim_{\beta \rightarrow 0} \bar{z} = \infty.$$

As a consequence, the proper minimal and maximal values for \bar{y} will be given by

$$\bar{y}_{min} = \lim_{\beta \rightarrow 0} \bar{y} = \frac{y_{PROD}}{k_1 + k_2}$$

and

$$\bar{y}_{max} = \lim_{\beta \rightarrow \infty} \bar{y} = \frac{y_{PROD}}{k_1 + k_2 \frac{u_0}{u_0 + p}}.$$

\bar{y} must behave as a continuous function of β between the limits considered, since \bar{z} in eq.(25) is a continuous function of β .

Consider now the effect of β on the coefficients A, B, C, D in (34)–(37) and, in turn, the effect of β on the parameters q, r in (46). By considering (34)–(37) together with the definition of g in (14) and the limits of \bar{y} , we arrive at the following limits for A, B, C, D :

$$\begin{aligned} \lim_{\beta \rightarrow 0} A(x, \beta) &= \infty, \\ \lim_{\beta \rightarrow \infty} A(x, \beta) &= A_{min} = A_0, \\ \lim_{\beta \rightarrow 0} B(\beta) &= B_{min} = \alpha_0 \left(a + b \frac{y_{PROD}}{k_1 + k_2} \right) - \theta, \\ \lim_{\beta \rightarrow \infty} B(\beta) &= B_{max} = \alpha_0 \left(a + b \frac{y_{PROD}}{k_1 + k_2 \frac{u_0}{u_0 + p}} \right) - \theta, \\ \lim_{\beta \rightarrow 0} C(\beta) &= C_{max} = \lim_{\beta \rightarrow 0} \frac{-k_2 p y_{PROD}}{(\bar{z}(\beta) + p)^2} = 0, \\ \lim_{\beta \rightarrow \infty} C(\beta) &= C_{min} = \frac{-k_2 p y_{PROD}}{(u_0 + p)^2 (k_1 + k_2 \frac{u_0}{u_0 + p})}, \\ \lim_{\beta \rightarrow 0} D(\beta) &= D_{min} = -(k_1 + k_2), \\ \lim_{\beta \rightarrow \infty} D(\beta) &= D_{max} = -(k_1 + k_2 \frac{u_0}{u_0 + p}). \end{aligned}$$

The coefficients A, B, C, D behave as continuous functions of β between the limits considered.

The properties of A, B, C, D imply that the scaled parameters q, r as defined in (38) behave as continuous functions of β' between definite limits. Since β' is scaled with respect to β by B , and B is positive with finite upper and lower limit, β' will tend to infinity in the same way as β . Consequently, coefficients q and r will be bounded between limits as follows:

$$0 < q < \frac{\frac{k_2 y_{PROD}}{(u_0 + p)^2 (k_1 + k_2 \frac{u_0}{u_0 + p})} \alpha_0 b u_0}{\left[\alpha_0 \left(a + b \frac{y_{PROD}}{k_1 + k_2 \frac{u_0}{u_0 + p}} \right) - \theta \right]^2}, \quad (61)$$

$$\frac{k_1 + k_2 \frac{u_0}{u_0 + p}}{\alpha_0 \left(a + b \frac{y_{PROD}}{k_1 + k_2 \frac{u_0}{u_0 + p}} \right) - \theta} < r < \frac{k_1 + k_2}{\alpha_0 \left(a + b \frac{y_{PROD}}{k_1 + k_2} \right) - \theta}, \quad (62)$$

with the denominators never being equal to zero because of the assumption $\alpha > 0$ mentioned earlier as a comment to (12).

6. Appendix B

It will be shown that the linearized, simplified system (39)–(44) is stable if the maturation rate β becomes large enough (the precise sense of which will become apparent later) while all other parameter values are kept fixed.

We apply an energy argument to show that with parameters $a, b, u_0, y_0, y_{PROD}, \alpha_0, k_1, k_2, p$ all fixed, we have:

$$\lim_{t \rightarrow \infty} \int_0^1 U^2(x, t) dx = 0,$$

and

$$\lim_{t \rightarrow \infty} Y^2(t) = 0.$$

The stability condition adopted here includes the condition $\lim_{t \rightarrow \infty} \int_0^1 |U(x, t)| dx = 0$, since only the L^1 norm of $U(\cdot, t)$ can be interpreted as a perturbation of the total cell count in the system. By using the Cauchy-Schwarz inequality, we get the estimate

$$\int_0^1 |U(x, t)| dx = \int_0^1 |U(x, t) \cdot 1| dx \leq \left[\int_0^1 |U(x, t)|^2 dx \right]^{\frac{1}{2}}$$

for all positive t . This means that we have the implication

$$\lim_{t \rightarrow \infty} \int_0^1 |U(x, t)|^2 dx = 0 \Rightarrow \lim_{t \rightarrow \infty} \int_0^1 |U(x, t)| dx = 0.$$

Let $\rho(x)$ be the function

$$\rho(x) = e^{-\frac{4x}{\beta}}, \quad x \in [0, 1],$$

and define E and F as functions of t by

$$E(t) = \int_0^1 \rho(x) U^2(x, t) dx, \quad F(t) = Y^2(t). \quad (63)$$

E and F are C^1 functions because of the assumed C^1 regularity of U and Y . (39) yields, together with the relation $U U_x = \frac{1}{2}(U^2)_x$:

$$\begin{aligned} \frac{d}{dt} \left(\frac{E(t)}{2} \right) &= \frac{d}{dt} \left[\frac{1}{2} \int_0^1 \rho(x) U^2(x, t) dx \right] = \int_0^1 \rho(x) U_t(x, t) U(x, t) dx \\ &= \int_0^1 \rho(x) [U(x, t) - q e^{\frac{x}{\beta}} Y(t)] U(x, t) dx \\ &\quad - \beta \int_0^1 \rho(x) \frac{1}{2} [U^2(x, t)]_x dx \\ &= E(t) - q Y(t) \int_0^1 \rho(x) e^{\frac{x}{\beta}} U(x, t) dx \\ &\quad - \beta \int_0^1 \rho(x) \frac{1}{2} [U^2(x, t)]_x dx. \end{aligned}$$

Looking closer at the last term above, we have by partial integration:

$$- \beta \int_0^1 \rho(x) \frac{1}{2} [U^2(x, t)]_x dx$$

$$\begin{aligned}
&= -\frac{\beta}{2}U^2(1, t)\rho(1) + \frac{\beta}{2}\int_0^1 \rho_x(x)U^2(x, t)dx \\
&= -\frac{\beta}{2}e^{-\frac{4}{\beta}}U^2(1, t) + \frac{\beta}{2}\int_0^1 \left(-\frac{4}{\beta}\right)e^{-\frac{4x}{\beta}}U^2(x, t)dx \\
&\leq -2\int_0^1 e^{-\frac{4x}{\beta}}U^2(x, t)dx = -2E(t).
\end{aligned}$$

With this inequality substituted into the equation above, we have:

$$\frac{d}{dt}(E(t)) \leq -2E(t) - 2qY(t)\int_0^1 \rho(x)e^{\frac{x}{\beta}}U(x, t)dx. \quad (64)$$

The Cauchy-Schwartz inequality applied to the last term in (64) yields:

$$\begin{aligned}
\left|\int_0^1 \rho(x)e^{\frac{x}{\beta}}U(x, t)dx\right| &= \left|\int_0^1 e^{\frac{x}{\beta}}\rho(x)^{\frac{1}{2}}\rho(x)^{\frac{1}{2}}U(x, t)dx\right| \\
&\leq \left[\int_0^1 (e^{\frac{x}{\beta}}\rho(x)^{\frac{1}{2}})^2 dx\right]^{\frac{1}{2}} \left[\int_0^1 (\rho(x)^{\frac{1}{2}}U(x, t))^2 dx\right]^{\frac{1}{2}} \\
&= \left[\frac{\beta}{2}(1 - e^{-\frac{2}{\beta}})\right]^{\frac{1}{2}} E(t)^{\frac{1}{2}}.
\end{aligned}$$

This inserted into inequality (64) above yields:

$$\frac{d}{dt}(E(t)) \leq -2E(t) + (2\beta)^{\frac{1}{2}}q(1 - e^{-\frac{2}{\beta}})^{\frac{1}{2}}E(t)^{\frac{1}{2}}|Y(t)|.$$

Hence, by using the general inequality $ab \leq \frac{1}{2}(a^2 + b^2)$:

$$\begin{aligned}
\frac{d}{dt}(E(t)) &\leq -2E(t) + \frac{1}{2}[E(t) + q^2 2\beta(1 - e^{-\frac{2}{\beta}})Y^2(t)] \\
&= -\frac{3}{2}E(t) + q^2\beta(1 - e^{-\frac{2}{\beta}})F(t).
\end{aligned} \quad (65)$$

By using (40) and the general inequality $ab = (\epsilon a)(\frac{b}{\epsilon}) \leq \frac{1}{2}[(\epsilon a)^2 + (\frac{b}{\epsilon})^2]$ we get, in the same way,

$$\frac{1}{2}\frac{d}{dt}[Y^2(t)] + rY^2(t) = Z(t)Y(t) \leq \frac{1}{2}\left[\frac{1}{r}Z^2(t) + rY^2(t)\right]. \quad (66)$$

Hence, by the Cauchy-Schwartz inequality,

$$\begin{aligned}
\frac{1}{2}\frac{d}{dt}[Y^2(t)] + \frac{1}{2}rY^2(t) &\leq \frac{1}{2r}Z^2(t) = \frac{1}{2r}\left(\int_0^1 \rho(x)^{-\frac{1}{2}}\rho(x)^{\frac{1}{2}}U(x, t)dx\right)^2 \\
&\leq \frac{1}{2r}\int_0^1 \rho(x)^{-1}dx \int_0^1 \rho(x)U^2(x, t)dx \\
&= \frac{1}{2r}\left(\int_0^1 e^{\frac{4x}{\beta}}dx\right)E(t).
\end{aligned}$$

The inequality above may be written in terms of $F(t) = Y^2(t)$:

$$\frac{d}{dt} F(t) \leq \frac{\beta}{4r} (e^{\frac{4}{\beta}} - 1) E(t) - r F(t). \quad (67)$$

Now, we have arrived at the two inequalities (65),(67) which are repeated below:

$$E_t(t) \leq -\frac{3}{2} E(t) + q^2 \beta (1 - e^{-\frac{2}{\beta}}) F(t), \quad (68)$$

$$F_t(t) \leq \frac{\beta}{4r} (e^{\frac{4}{\beta}} - 1) E(t) - r F(t). \quad (69)$$

Next, we multiply inequality (69) by the factor $k(\beta) = \frac{1}{\frac{\beta}{4r}(e^{\frac{4}{\beta}} - 1)}$ and add (68),(69) together to yield:

$$E_t(t) + k(\beta) F_t(t) = -\frac{1}{2} E(t) + p(\beta) F(t) \quad (70)$$

where $p(\beta)$ is defined by

$$p(\beta) = q^2 \beta (1 - e^{-\frac{2}{\beta}}) - r k(\beta). \quad (71)$$

This implies

$$\begin{aligned} E_t(t) + k(\beta) F_t(t) &= -\frac{1}{2} E(t) + \frac{p(\beta)}{k(\beta)} k(\beta) F(t) \\ &\leq \max\left[-\frac{1}{2}, \frac{p(\beta)}{k(\beta)}\right] [E(t) + k(\beta) F(t)]. \end{aligned} \quad (72)$$

If we can assume that $\frac{p(\beta)}{k(\beta)} < 0$, then by Gronwall's inequality [37], this implies

$$E(t) + k(\beta) F(t) \leq e^{\epsilon t} [E(0) + k(\beta) F(0)],$$

where $\epsilon = \max\left[-\frac{1}{2}, \frac{p(\beta)}{k(\beta)}\right]$ is a negative number. This means that $E(t) + k(\beta) F(t)$ will approach zero as $t \rightarrow \infty$. Thus, since $E(t)$, $F(t)$, and $k(\beta)$ are all positive, $E(t)$ and $F(t)$ must tend to zero individually and the perturbations $\int_0^1 U^2(x, t) dx$ and $Y^2(t)$ must likewise approach zero since the weighting function $\rho(x)$ is positive for all x . As shown initially in this appendix, this also means that $U(x, t)$ approaches zero in the L^1 norm. Hence, the system (39)–(44) is stable in this sense.

It remains to state explicitly the condition that the function $p(\beta)$ defined in (71) is negative-valued. According to the definition, $p(\beta) < 0$ implies

$$q < \frac{2r}{\beta \sqrt{(1 - e^{-\frac{2}{\beta}})(e^{\frac{4}{\beta}} - 1)}}. \quad (73)$$

The function of β on the right-hand side of this inequality defined as

$$\sigma_r(\beta) = \frac{2r}{\beta \sqrt{(1 - e^{-\frac{2}{\beta}})(e^{\frac{4}{\beta}} - 1)}} \quad (74)$$

is a strictly increasing function of β at constant r (Figure 6). This means that at constant r and q , the system will be stable if β is chosen large enough in the sense of satisfying condition (73). On the other hand, with a given value of β and r , the system is stable if q is chosen small enough to satisfy (73). Especially, the system is stable as $\beta \rightarrow \infty$ if r and q are functions of β as given by the physiological interpretation. This is due to the fact that r and q are bounded between finite limits as shown in Appendix A (61),(62), while the function $\sigma_r(\beta)$ becomes unbounded for large β .

References

1. Aglietta, M., Piacibello, W., Sanavio, F., Stacchini, A., Aprá, F., Schena, M., Mossetti, C., Carnino, F., Caligaris-Cappio, F., Gavosto, F.: Kinetics of human hemopoietic cells after in vivo administration of granulocyte-macrophage colony-stimulating factor. *J. Clin. Invest.* **83**, 551–557 (1989)
2. Apostol, T.M.: *Mathematical analysis*. Addison-Wesley, Reading Massachusetts Palo Alto London, 1965, pp. 146–148
3. Benestad, H.B., Rytömaa, T.: Regulation of maturation rate of mouse granulocytes. *Cell Tissue Kinet* **10**, 461–468 (1977)
4. Brandt, L., Forssman, O., Mitelman, F., Odeberg, H., Olofsson, T., Olsson, I., Svensson, B.: Cell production and cell function in human cyclic neutropenia. *Scand. J. Haematol.* **15**, 228–240 (1975)
5. Denkers, I.A.M., Dragowska, W., Jaggi, B., Palcic, B., Lansdorp, P.M.: Time lapse video recordings of highly purified human hematopoietic progenitor cells in culture. *Stem Cells* **11**, 243–248 (1993)
6. Driver, R.D.: *Ordinary and Delay Differential Equations*. Springer, New York, 1977
7. Frick, P.: *Blut- und Knochenmarksmorphologie: Blutgerinnung*. Georg Thieme Verlag 16. Aufl., Stuttgart New York 1982
8. Gurtin, M.E., MacCamy, R.C.: Non-linear age-dependent population dynamics. *Arch. Rat. Mech. Anal.* **54**, 381–300 (1974)
9. Hammond, W.P., Chatta, G.S., Andrews, R.G., Dale, D.C.: Abnormal responsiveness of granulocyte-committed progenitor cells in cyclic neutropenia. *Blood* **79** (10), 2536–2539 (1992)
10. Hammond, W.P., Price, T.H., Souza, L.M., Dale, D.C.: Treatment of cyclic neutropenia with granulocyte colony-stimulating factor. *N. Engl. J. Med.* **320**, 1306–11 (1989)
11. Hammond, W.P., Boone, T.C., Donahue, R.E., Souza, L.M., Dale, D.C.: Comparison of treatment of canine cyclic hematopoiesis with recombinant human granulocyte-macrophage colony stimulating factor(GM-CSF), G-CSF, Interleukin-3, and Canine G-CSF. *Blood* **76**, 523 (1990)
12. Haurie, C., Dale, D.C., Mackey, M.C.: Cyclical neutropenia and other periodic hematological disorders: A review of mechanisms and mathematical models. *Blood* **8**, 2629–2640 (1998)
13. Haurie, C., Dale, D.C., Mackey, M.C.: Occurrence of periodic oscillations in the differential blood counts of congenital, idiopathic, and cyclical neutropenic patients before and during treatment with G-CSF. *Exp. Hematol.* **27**, 401–409 (1999)
14. Haurie, C., Person, R., Dale, D.C., Mackey, M.C.: Hematopoietic dynamics in grey collies. *Exp. Hematol.* **27**, 1139–1148 (1999)
15. Haurie, C., Dale, D.C., Rudnicki, R., Mackey, M.C.: Modeling complex neutrophil dynamics in the grey collie. *J. Theor. Biol.* **204**, 505–519 (2000)

16. Jacobsen, N., Broxmeyer, H.: Oscillations of granulocytic and megakaryocytic progenitor cell populations in cyclic neutropenia in man. *Scand. J. Haematol.* **23**, 33–36 (1979)
17. Kaplan, J.L., Yorke, J.A.: On the stability of a periodic solution of a differential delay equation. *SIAM J. Math. Anal.* **6** (2), 268–282 (1975)
18. King-Smith, E., Morley, A.: Computer simulation of granulopoiesis: Normal and impaired granulopoiesis. *Blood* **36** (2), 254–262 (1970)
19. Kvalheim, G.: Clinical use of enriched CD34+ cells. *Blood Therapies in Medicine* **2** (2), 57–64 (2002)
20. Lebowitz, J.L., Rubinow, S.I.: A mathematical model of neutrophil production and control in normal man. *J. Math. Biol.* **1**, 187–225 (1975)
21. MacDonald, N.: *Biological delay systems: Linear stability theory*. Cambridge University Press, Cambridge, 1989
22. Glass, L., Mackey, M.C.: Pathological conditions resulting from instabilities in physiological control systems. *Ann. N. Y. Acad. Sci.* **316**, 214–235 (1979)
23. Mackey, M.C., Glass, L.: Oscillation and chaos in physiological control systems. *Science* **197**, 287–289 (1977)
24. Mackey, M.C., Milton, J.G.: Feedback, delays and the origin of blood cell dynamics. *Comm. Theor. Biol.* **1**, 299–327 (1990)
25. Mahaffy, J.M., Belair, J., Mackey, M.C.: Hematopoietic model with moving boundary condition and state dependent delay: Applications in erythropoiesis. *J. Theor. Biol.* **190**, 135–146 (1998)
26. Mahaffy, J.M.: A test for stability of linear differential delay. equations. *Quart. Appl. Math.*, July, 193–202 (1982)
27. Morley, A., Stohlman, F.: Studies on the regulation of granulopoiesis. I. The response to neutropenia. *Blood* **35** (3), 312–321 (1970)
28. Murray, J.D.: *Mathematical Biology*. Springer-Verlag, New York Berlin Heidelberg, 1989
29. Lagarias, J.C., Reeds, J.A., Wright, M.H., Wright, P.E.: Convergence properties of the Nelder-Mead simplex method in low dimensions. *SIAM J. Optim.* **9** (1), 112–147 (1998)
30. Schmitz, S., Franke, H., Loeffler, M., Wichmann, H.E., Diehl, V.: Reduced variance of bone-marrow transit time of granulopoiesis - a possible pathomechanism of human cyclic neutropenia. *Cell Prolif* **27**, 655–667 (1994)
31. Schmitz, S., Franke, H., Loeffler, M., Wichmann, H.E., Diehl, V.: Model analysis of the contrasting effects of GM-CSF and G-CSF treatment on peripheral blood neutrophils observed in three patients with childhood-onset cyclic neutropenia. *Brit. J. Haematol.* **95**, 616–625 (1996)
32. Schmitz, S., Franke, H., Wichmann, H.E., Diehl, V.: The effect of continuous G-CSF application in human cyclic neutropenia: a model analysis. *Brit. J. Haematol.* **90**, 41–47 (1995)
33. Schmitz, S., Franke, H., Brusis, J., Wichmann, H.: Quantification of the cell kinetic effects of G-CSF using a model of human granulopoiesis. *Exp. Hematol.* **31**, 755–760 (1993)
34. Schmitz, S., Franke, H., Wichmann, H.E., Diehl, V.: The effect of continuous G-CSF application in human cyclic neutropenia: a model analysis. *Brit. J. Haematol.* **90**, 41–47 (1995)
35. Von Schultess, G.K., Mazer, N.A.: Cyclic neutropenia: A clue to the control of granulopoiesis. *Blood* **59** (1), 27–37 (1982)
36. Tibken, B., Hofer, E.P.: A biomathematical model of granulocytogenesis for estimation of stem cell numbers. *Stem Cells* **13**(suppl 1), 283–289 (1995)
37. Tveito, A., Winther, R.: *Introduction to partial differential equations*. Springer-Verlag, New York Berlin Heidelberg, 1998

38. Warner, H.R., Athens, J.W.: An analysis of granulocyte kinetics in blood and bone marrow. *Ann. N. Y. Acad. Sci.* **113**, 523–536 (1964)
39. Wichmann, H.E., Loeffler, M., Schmitz, S.: A concept of hemopoietic regulation and its biomathematical realization. *Blood Cells* **14**, 411–429 (1988)
40. Wright, D.G., LaRussa, V., Salvado, A.J., Knight, R.D.: Abnormal responses of myeloid progenitor cells to granulocyte-macrophage colony-stimulating factor in human cyclic neutropenia. *J. Clin. Invest.* **83**, 1414–1418 (1989)
41. Østby, I., Rusten, L.S., Kvalheim, G., Grøttum, P.: A mathematical model for reconstitution of granulopoiesis after high dose chemotherapy with autologous stem cell transplantation. *J. Math. Biol.* **47**, 101–136 (2003) DOI 10.1007/s00285-003-0198-6